

Preparation and Characterizations of Nano-TiO₂ Reinforced Poly Ethylene Oxide Nanocomposite Films – Optical and DC Conductivity Properties

K. Sudhakar¹, R. Venugopal¹, N. Narsimlu² and CH. Srinivas^{2*}

¹Dept. of Physics, UCS, Osmania University, Hyderabad, Telangana State, India.

²Dept. of Physics, UCE(A), Osmania University, Hyderabad, Telangana State, India.

Abstract:

The solution casting method had been used to prepare PEO/TiO₂ nanocomposites films reinforced with different wt% (5,10,15) of Nano-TiO₂. The XRD studies revealed that the appearance of intensity peaks at 32° and 43° in PEO/TiO₂ nanocomposites suggest the incorporation of Nano-TiO₂ into pure PEO and formation of different ordered phases in small domains. SEM studies revealed that the percentage of dark regions is higher compared to bright regions in higher wt% of Nano-TiO₂ Nanocomposites, which revealed a degradation in crystallinity of Nanocomposite films. The noticeable porous structures in SEM micrographs, may act as conducting pathways for ions from cathode to anode or vice-versa, supporting enhancement of ionic conductivity in PEO/TiO₂ Nanocomposite films. FTIR studies established the incorporation of Nano-TiO₂ particles into the PEO matrix. UV-Vis studies exhibit the absorption edge of the Nanocomposite films was moved from ~ 235 nm (for pure PEO) to ~ 262 nm (for 15 wt% Nano-TiO₂ reinforced PEO) films. The absorption edge of Nanocomposite films shift to a longer wavelength, within UV region, with increment of Nano-TiO₂ wt% i.e., Nanocomposites act as UV absorber. The indirect bandgap energy value decreased from 5.51 eV (for pure PEO) to 5.29 eV (for 5 wt% Nano-TiO₂ reinforced PEO - Nanocomposite). Whereas the direct bandgap energy has been decreased from 5.38 eV (for pure PEO) to 5.06 eV (for 15 wt% Nano-TiO₂ reinforced PEO – Nanocomposite). Urbach energy values decreased with increasing wt% of Nano-TiO₂. The DC conductivity with temperature variation from 30°C to 80°C, which is slightly above the melting temperature of the PEO polymer host, were studied. The Conductivity (σ) is jumped at a temperature of ~ 65 °C, which correspond to phase transition of PEO polymer from semicrystalline phase to amorphous phase.

Key- Words: Reinforced, Hybrid materials, Nano-TiO₂, PEO/TiO₂ Nanocomposites, Optical properties.

Date of Submission: 09-10-2023

Date of Acceptance: 19-10-2023

I. Introduction

Polymers reinforced with Nanofillers result into a class of hybrid materials known as Polymer Nanocomposites. The properties of polymer nanocomposites depend on the size, structure and type of fillers that incorporated into polymers. These materials exhibit unique properties pertaining to hardness, thermal stability, electrical conductivity, absorption of UV radiation in particular based on type Nanofillers incorporated. The Nanofillers may be classified into a class of inorganic particles and organic particles. The Inorganic nanofillers have a large surface area which give an advantage of increase in interfacial area on incorporation into polymers, which resulted into many many applications [1].

In the present paper, Poly (ethylene Oxide) (PEO) has been considered base matrix polymer. It is one of the prominent polymer due to its high chemical and thermal stability, possess semi-crystalline nature. The average molecular weight of PEO is 10⁵ and completely soluble in water at room temperature. In the multiphase character of PEO, the amorphous phase exhibit conductivity based on ionic conduction [2]. PEO has been widely used in various applications due to its ability to surface modification on incorporation of inorganic oxide nanoparticles, which enhance their size, shape, solubility, long-term stability and attachment to selective functional group [3, 4, 5].

In present work, Titanium Dioxide (TiO₂) has been used as inorganic Nanofiller. TiO₂ is commonly used as a photocatalyst in water decontamination process due to its efficiency, stability, low toxicity and cost effectiveness [6, 7, 8]. But it has limitations, such as a large band gap energy.

In this paper, the preparation and characterization of PEO/TiO₂ Nanocomposites with incorporation of different wt% (5,10,15) of Nano-TiO₂ has been presented. The prepared nanocomposites are subjected to X-Ray Diffraction (XRD), Scanning Electron Microscopy (SEM), Fourier Transform Infrared (FTIR)

Spectroscopy Studies, UV/Visible Spectroscopy, Temperature dependency of DC conductivity. These studies explore the structural, morphological, DC conductivity and UV absorption of PEO/TiO₂Nanocomposites.

II. Experimental

Materials and methods

Poly Ethylene Oxide (amv: 1,00,000, fp - 229°C) was procured from Sigma Aldrich, India. Titanium dioxide nanoparticles (average particle size 30-50 nm, purity > 99%) was procured from Ad-NanoTechnologiesPtv. Ltd. High quality Petri dishes (Polypropylene) (dia- 60mm) from Polylab, Double Distilled water, Magnetic Stirrer.

Preparation of Nanocomposites

By using effective *Solution Casting method* of preparation, pure Polyethylene Oxide (PEO) and Nano-TiO₂ incorporated PEO i.e., PEO/TiO₂Nanocomposite films had been prepared. 3g of PEO was dissolved in double distilled water (70ml) and magnetically stirred (600 rpm) for 48 hours at ambient temperature resulted into homogenous viscous solution of PEO, such four separate solutions were prepared. One of them was transferred into *petridish*and ensure that there was no air bubbles in the solution for pure PEO base matrix film.

TiO₂ nanoparticles were dispersed into double distilled water (30ml) with wt% of 5, 10, 15 (Table-1) separately and magnetically stirred (600 rpm) for 6 hours at ambient temperature. Subsequently the respective dispersed different wt% of Nano-TiO₂ were added to above prepared remaining three PEO solutions, these three samples are magnetically stirred (600rpm) separately for 48 hours at ambient temperature. The resulted PEO/TiO₂nanocomposite solutions of 5,10,15wt% of Nano-TiO₂ are transferred into petridishesand allowed to natural drying at ambient temperature. After around four weeks, Pure PEO film and three PEO/TiO₂Nanocomposite films were obtained as per Table1.

Table-1. Compositions of Nano-TiO₂and PEO/TiO₂ Nanocomposite films

S. No	Sample	Values of x (wt.%)	Contents of PEO (g)	Nano-TiO ₂ (g)
1	PPE0 (Pure PEO)	0	3	0
2	TP05 (PEO/5 Wt% TiO ₂)	5	3	0.15
3	TP10 (PEO/10 Wt% TiO ₂)	10	3	0.3
4	TP15 (PEO/15 Wt% TiO ₂)	15	3	0.45

Characterizations

The structural characteristics of PEO/TiO₂nanocomposite thin films were conducted using an X-ray diffractometer (Bruker D-8 Advance) with Cu (K_α) having the wavelength 1.5406 Å. With a 30 kV accelerating voltage, The surface morphology was studied using a Scanning Electron Microscope (SEM) (Quanta250 FEG FEI). The samples were coated with a 3.5 nm gold layer to reduce the charging effects of the electron beam.

The Fourier Transform Infrared (FTIR) spectroscopy of the nanocomposites was recorded using a SHIMADZU-8400S spectrometer in transmission mode with a resolution of 4 cm⁻¹. The UV absorption data of the nanocomposite films was obtained using a UV-Vis spectrophotometer(SHIMADZU UV-1800 Series) operating in the 190-1100nm wavelength range. The DC electrical conductivity tests were performed using a four-probe electrical conductivity System equipped with a thermal chuck.

III. Results and Discussions

(i) XRDAnalysis :

Figure 1 represents X-ray spectra for pure PEO and PEO-TiO₂nanocomposite films with different wt% of TiO₂. Pure PEO shows its characteristic maximum intensity peaks at (2θ=) 23° and following maximum intensity peak at 19°, they are assigned to (112) and (120) planes of crystalline PEO respectively [PCPDF File number 49-2200].

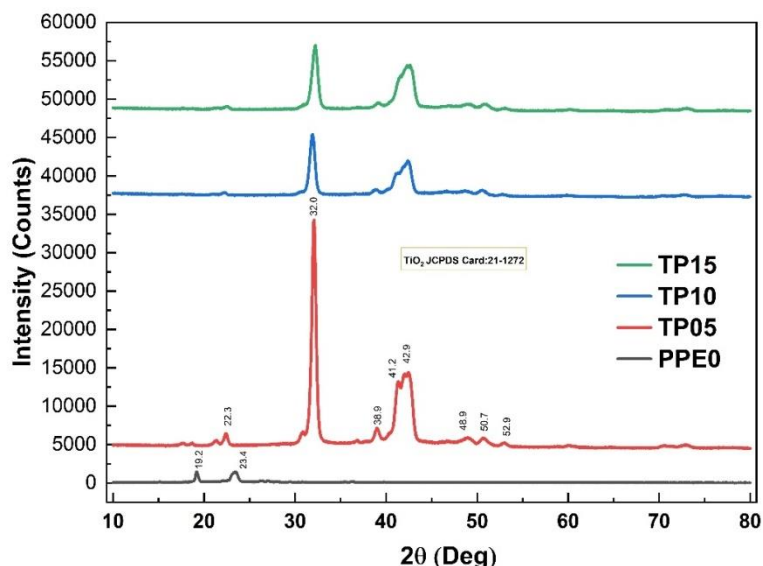


Figure 1 XRD Patterns of pure PEO and PEO/TiO₂Nanocomposite films

The considerable reduction of intensity for PEO-(xwt%)TiO₂nanocomposite films (x=5, 10, 15 wt%) at 19° and 23° confirms the incorporation of TiO₂ into PEO matrix, which is responsible for reduction in crystalline phase of PEO. This reduction in intensity has been pronounced more as increment of wt % of TiO₂[10].

The appearance of intensity peaks at 32° and 43° in PEO/TiO₂nanocomposite films suggests the incorporation of TiO₂ nanoparticles and formation of different ordered phases in small domains due to this incorporation of TiO₂ nanoparticles into PEO matrix. This also confirms heterogeneous nucleation of TiO₂ nanoparticles, which influence on the crystalline region of Pure PEO matrix reduces to semicrystalline nature. Peaks associated with Pure PEO can also be observed in the PEO/TiO₂nanocomposite films, hence, there are two phases i.e., crystalline phase and more pronounced semicrystalline phase, within PEO/TiO₂nanocomposite films [11].

(ii) SEM analysis - Surface Morphology :

Figure 2 represents Scanning Electron Micrographs of Pure PEO and PEO/TiO₂Nanocomposite films. Various bright and dark regions can be observed from the micrographs. Figure 2.2 revealed EDAX for elemental compositions of nanocomposites.

In PEO/TiO₂Nanocomposite films, the bright regions with spherulites assigned to the crystalline phase of PEO and dark regions represent the amorphous phase of the PEO in PEO/TiO₂Nanocomposite films. In PEO/TiO₂Nanocomposite films, from SEM images, the percentage of dark regions is higher compared to bright regions, which revealed a degradation in crystallinity of Nanocomposite films. The noticeable porous structures in SEM micrographs, may act as conducting pathways for ions from cathode to anode or vice-versa, supporting enhancement of ionic conductivity in PEO/TiO₂Nanocomposite films [12].

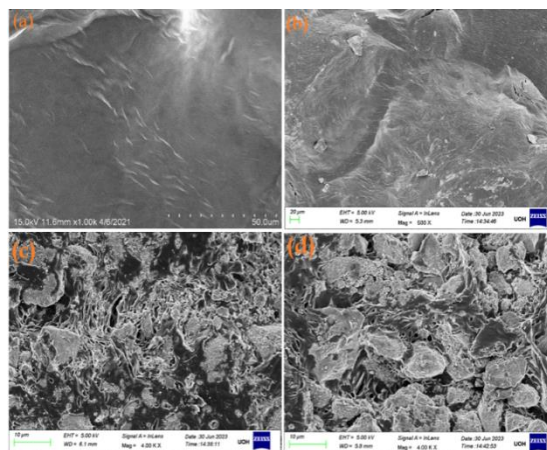


Fig.2 SEM images of pure PEO and PEO-TiO₂ nanocomposite films

(iii) Fourier Transform Infrared (FTIR) Spectroscopy Studies :

Figure 3 shows FTIR spectra of Pure PEO, PEO/TiO₂Nanocomposites with 5, 10, 15 Wt% of Nano-TiO₂ reinforcement. The peak positions of various functional groups in pure PEO and their associated vibrational modes were presented in Table 2, the results were in correspondence with other literature reports [13].

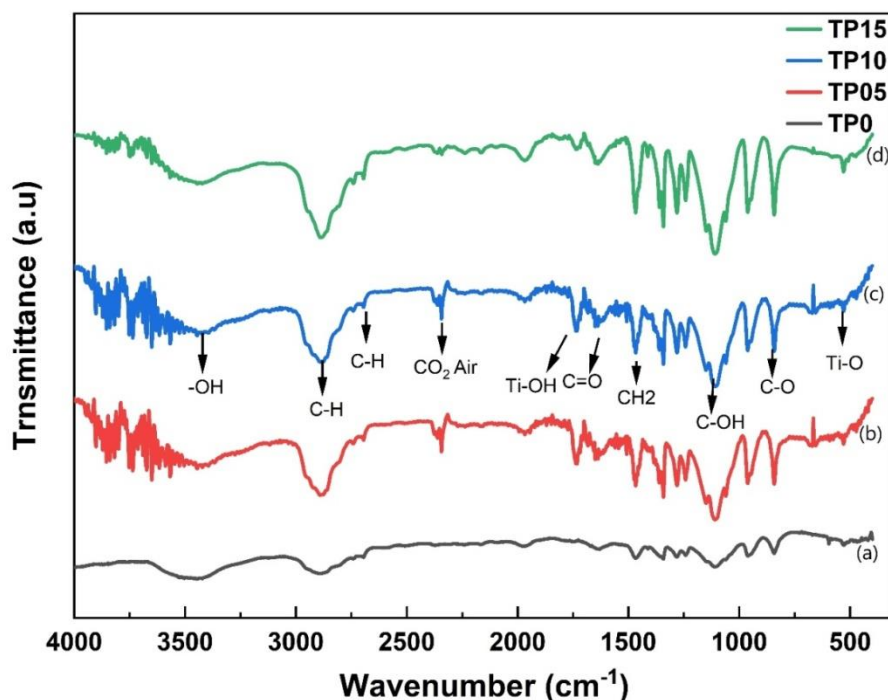


Fig.3 Fourier transform infrared (FTIR) spectra of nano-TiO₂ incorporated PEO nanocomposite films.

Table-2.Characteristic vibration bands observed in PEO-TiO₂nanocomposite films.

Vibrational modes	Corresponding peak positions (cm ⁻¹)
O-Ti-O	531
C-C (out-of-plane vibration)	844
C-O (stretching)	939
C-OH (stretching)	1074
C-H Wagging	1245
CH ₂ (bending)	1430
C=O stretching	1734
CO ₂ air	2189
C-H stretching	2924
-OH stretching	3330

Nano-TiO₂ reinforced into PEO matrix with 5, 10, 15 wt% FTIR spectra had been presented. It was evident from the results, the slight shift for the peak position corresponding to C-OH stretching mode from 1074 cm⁻¹ to 1090 cm⁻¹ for the PEO/TiO₂Nanocomposite (reinforced with 10 Wt% of nano-TiO₂). The vibrational peaks corresponding to C=O stretching at 1734 cm⁻¹ and O-H stretching mode at 3330 cm⁻¹ seem to be narrower after loading TiO₂ into PEO i.e., shifting the edges of peaks. It can be attributed to the dissociation of hydrogen bonds present in PEO due to reinforcement of Nano-TiO₂ in PEO matrix.

The low wavenumber peak at 531 cm⁻¹ was observed, it can be attributed to O-Ti-O vibration. In fact, the vibrational modes of bands in PEO were affected by incorporation of TiO₂ due to the establishment of new hydrogen bonding, between -OH groups of PEO and TiO₂. These observations emphatically confirms the interaction of PEO with Nano-TiO₂ and reinforcement of TiO₂ into PEO matrix [14].

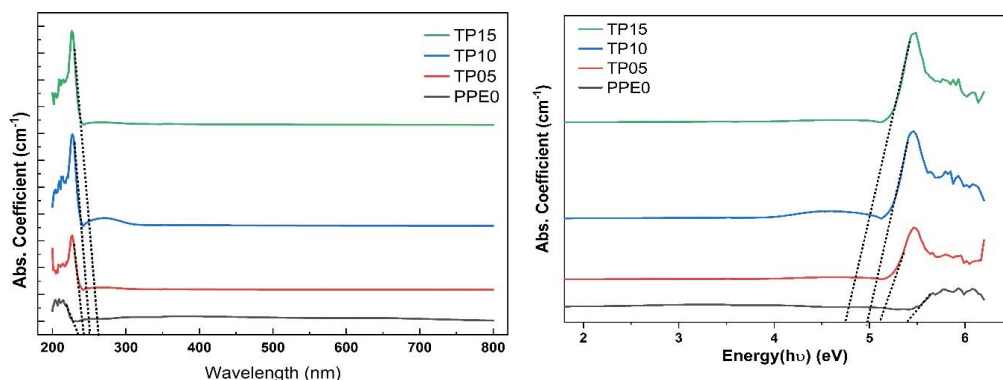
(iv). UV-Vis Spectroscopy – Optical properties :**(a) Optical Absorbance**

Fig. 4 Variation of abs. coefficient with the wavelength and energy for pure PEO and PEO/TiO₂ nanocomposite films

The significant trend of increase in absorbance of the PEO/TiO₂ Nanocomposite film increases as the wavelength decreases. This trend is more pronounced as the wt% of Nano-TiO₂ increment in PEO. Hence, PEO/TiO₂ Nanocomposite films exhibit good UV radiation protection properties.[15,16].

The absorption edge of the Nanocomposite films was moved from ~ 235 nm (for pure PEO) to ~ 262 nm (for 15 wt% Nano-TiO₂ reinforced PEO) films. The absorption edge of Nanocomposite films shift to a longer wavelength with increment of Nano-TiO₂ wt%, which indicates the amorphous nature of PEO/TiO₂ nanocomposite and formation of bonds among TiO₂ and PEO matrix due to hydrogen bonding between Nano-TiO₂ and –OH group of PEO [17, 18, 19]. The absorption edge values, in-terms of energy and wavelength, were tabulated in Table 3.

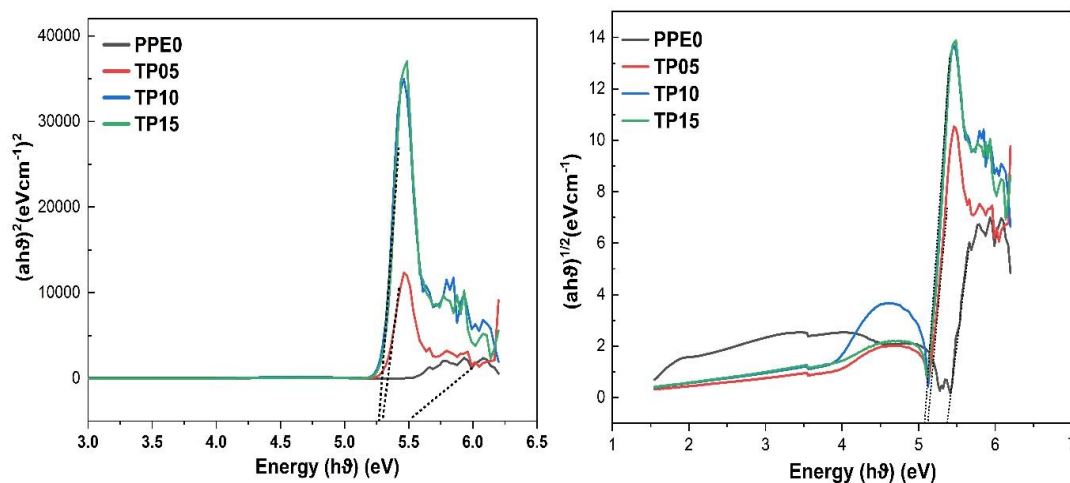
(b) Direct and Indirect bandgap energy

Fig.5 Variation of (a) direct and (b) indirect bandgap as a function of energy for pure PEO and PEO/TiO₂ nanocomposite films

Figure 5 shows the Tauc plots for direct and indirect bandgap energy for pure PEO and PEO/TiO₂ nanocomposites. As per Tauc equation, $(\alpha h\nu)^n = k (h\nu - E_g)$; if $n=1/2$ for allowed indirect bandgap transition and $n=2$ for allowed direct bandgap transition [20].

The indirect bandgap energy value decreased from 5.51 eV (for pure PEO) to 5.29 eV (for 5 wt% Nano-TiO₂ reinforced PEO - Nanocomposite). Whereas the direct bandgap energy has been decreased from 5.38 eV (for pure PEO) to 5.06 eV (for 15 wt% Nano-TiO₂ reinforced PEO – Nanocomposite). The direct and indirect bandgap energy values are tabulated in Table 3.

It is evident that increasing wt% of Nano-TiO₂ reinforcement within PEO shifts the direct and indirect bandgap energy values to lower values, it may be due to induced additional local defects by TiO₂ nanoparticles

in the PEO matrix alter the states in the optical band which intern later the valence and conduction band edges. This could be the prime reason for the bandgap reduction in Nanocomposites [21].

(c) Urbach energy

The bandgap energy of amorphous and semicrystalline materials can be calculated using the Urbach relation. The Urbach energy (E_u) is evaluated using the following equation[22].

$$\log \alpha = \log c + \frac{hv}{E_u}$$

Where c is a constant, the band tail energy or the Urbach energy (E_u) can be obtained from the slope of the line of the graph ln(α) as a function of incident photon energy (hv).

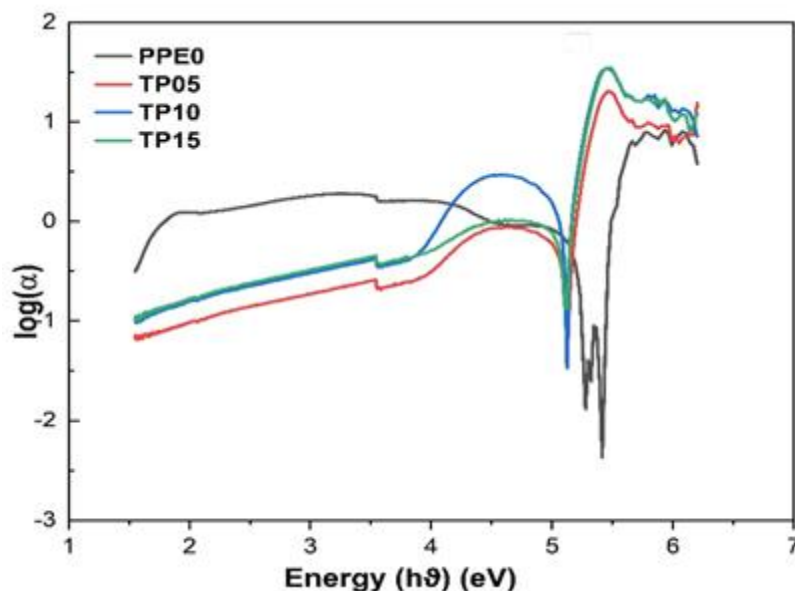


Figure 6. Urbach energy of pure PEO and PEO/TiO₂ nanocomposite films

The Urbach energy values for pure PEO and different wt% of Nano-TiO₂ reinforced PEO matrix were tabulated in Table 3. Urbach energy values decreased with increasing wt% of Nano-TiO₂. It may be due to indicating a slightly enhanced crystallization and disturbance of phonon state in polymer nanocomposites, impurity level in the middle of optical bandgap, structure disorder, inhomogeneous strain [23].

Table3. Absorption edge; Direct, Indirect bandgap and Urbach energy values of pure PEO and PEO-TiO₂ composite films:

S.NO	Composite	Absorption edge(eV)	Absorption edge(nm)	Direct bandgap (eV)	Indirect bandgap (eV)	Urbach energy (eV)
1	PPE0 (Pure PEO)	5.40	235	5.51	5.38	5.82
2	TP05 (PEO/5 Wt% TiO ₂)	5.12	242	5.29	5.12	4.96
3	TP10 (PEO/10 Wt% TiO ₂)	4.97	250	5.26	5.08	4.95
4	TP15 (PEO/15 Wt% TiO ₂)	4.74	262	5.24	5.06	4.95

(v) Temperature dependence of DC Conductivity:

Figure 7 shows the Temperature-dependent ionic conductivity for different PEO/TiO₂ Nanocomposite films. The temperature were varied from 30°C to 80°C, which is slightly above the melting temperature of the PEO polymer host. The ionic conductivity of the different Nanocomposite films linearly increases with the temperature.

The Plot of 'Log σ_{dc} vs. 1000/T' i.e., Figure 8, shows a linear increase in conductivity as a function of

temperature. There is an Arrhenius-type behavior given by the general equation:

$$\sigma(T) = \sigma_0 \exp(-E_a/kT)$$

Where σ_0 = pre-exponential factor; E_a = activation energy.

k = Boltzmann constant and T = temperature in Kelvin

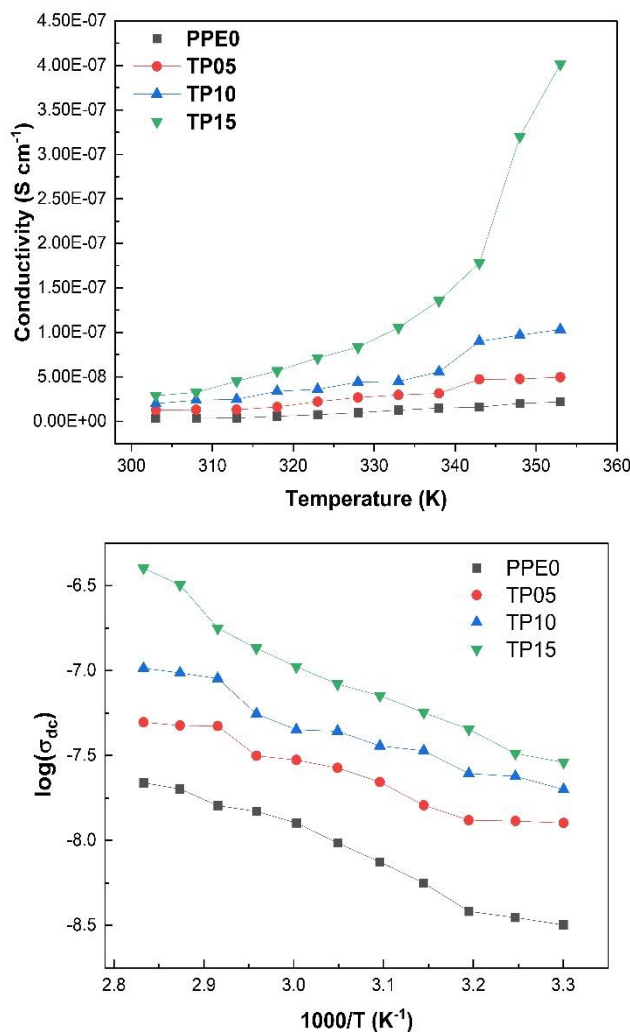


Fig. 8 $\log \sigma_{dc}$ vs. $1000/T$ plot for PEO-TiO₂ Nanocomposites with different wt.% compositions.

The increase in ionic conductivity with temperature may possibly due to an increase in ionic mobility or carrier ions' concentration. Conductivity (σ) jump is observed at a temperature of ~ 65 °C, which corresponds to phase transition of PEO polymer from semicrystalline phase to amorphous phase. Due to phase change of host polymer, the conductivity suddenly increases at melting temperature T_m . The rise in conductivity as a function of temperature may also be attributable to a process of hopping between coordinating locales, local structural relaxations, and the segmental motions of the polymer PEO[24]. The curve fitting of the linear portion below this temperature follows the Arrhenius Equation.

For PEO/TiO₂ Nanocomposite films, the Arrhenius equation is $\sigma(T) = 4.94 \times 10^{-4} \exp(-0.814/kT)$

It can be seen from the above equation that the numerator in the argument of the exponential is an activation energy $E_a = 0.814$ eV. The relationship between activation energy E_a and concentration of Nano-TiO₂ particles presented in Fig.9. It can be seen from Fig.9 that activation energy is minimum for $x = 5$ wt.% of TiO₂. The low activation energy (E_a) of PEO/TiO₂ Nanocomposite films confirms the high ionic conductivity of the composition.

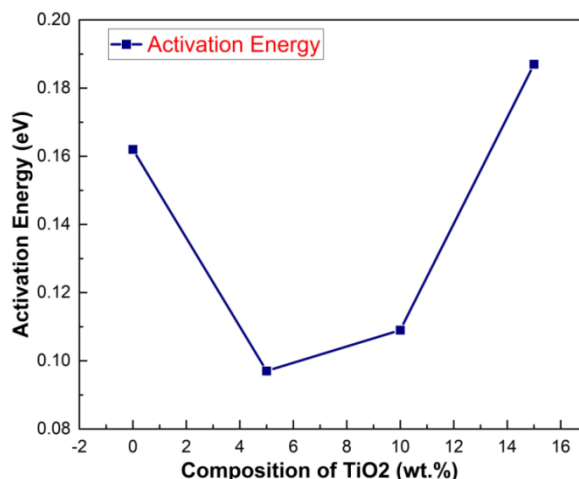


Fig. 9 Activation energy E_a vs Composition of TiO₂ for PEO-TiO₂ nanocomposites.

IV. Conclusions

The cost-effective technique of solution casting method was used to prepare PEO/TiO₂ Nanocomposite films with different wt% (5,10,15) of Nano-TiO₂, which were found to be semicrystalline in nature through XRD studies. The XRD studies revealed that the appearance of intensity peaks at 32° and 43° in PEO/TiO₂ nanocomposites suggest the incorporation of Nano-TiO₂ into pure PEO and formation of different ordered phases in small domains.

The SEM studies indicated that the film surface is smooth at the lower wt% of Nano-TiO₂, and the surface roughness of the films increased with the increase of wt% of Nano-TiO₂. The SEM studies also revealed that the percentage of dark regions is higher compared to bright regions in higher wt% of Nano-TiO₂ Nanocomposites, which revealed a degradation in crystallinity of Nanocomposite films. The noticeable porous structures in SEM micrographs, may act as conducting pathways for ions from cathode to anode or vice-versa, supporting enhancement of ionic conductivity in PEO/TiO₂ Nanocomposite films. FTIR studies established the incorporation of Nano-TiO₂ particles into the PEO matrix.

UV-Vis studies exhibit the absorption edge of the Nanocomposite films was moved from ~ 235 nm (for pure PEO) to ~ 262 nm (for 15 wt% Nano-TiO₂ reinforced PEO) films. The absorption edge of Nanocomposite films shift to a longer wavelength, within UV region, with increment of Nano-TiO₂ wt% i.e., Nanocomposites act as UV absorber. The indirect bandgap energy value decreased from 5.51 eV (for pure PEO) to 5.29 eV (for 5 wt% Nano-TiO₂ reinforced PEO - Nanocomposite). Whereas the direct bandgap energy has been decreased from 5.38 eV (for pure PEO) to 5.06 eV (for 15 wt% Nano-TiO₂ reinforced PEO - Nanocomposite). Urbach energy values decreased with increasing wt% of Nano-TiO₂. It may be due to, indication of slightly enhanced crystallization and disturbance of phonon state in polymer nanocomposites, impurity level in the middle of optical bandgap, structure disorder, inhomogeneous strain. The DC conductivity with temperature variation from 30°C to 80°C, which is slightly above the melting temperature of the PEO polymer host, were studied. The Conductivity (σ) is jumped at a temperature of ~ 65 °C, which correspond to phase transition of PEO polymer from semicrystalline phase to amorphous phase.

References

- [1]. Vashisth, A., Kowalik, M., Gerringer, J., Ashraf, C., Duin, A. C. T. V., & Green, M. J. (2020). Reaxff Simulations Of Laser-Induced Graphene (Lig) Formation For Multifunctional Polymer Nanocomposites. *ACS Applied Nano Materials*, 3(2), 1881-1890. <https://doi.org/10.1021/acsanm.9b02524>
- [2]. Yoo, D. H., Cuong, T. V., Pham, V. H., Chung, J. S., Khoa, N. T., Kim, E. J., & Hahn, S. H. (2011). Enhanced Photocatalytic Activity Of Graphene Oxide Decorated On TiO₂ Films Under UV And Visible Irradiation. *Current Applied Physics*, 11(3), 805-808. <https://doi.org/10.1016/j.cap.2010.11.077>
- [3]. Zhao, B., Macminn, C. W., & Juanes, R. (2016). Wettability Control On Multiphase Flow In Patterned Microfluidics. *Proceedings Of The National Academy Of Sciences*, 113(37), 10251-10256. <https://doi.org/10.1073/pnas.1603387113>
- [4]. Li, Y., Rodrigues, J. D., & Tomás, H. (2012). Injectable And Biodegradable Hydrogels: Gelation, Biodegradation And Biomedical Applications. *Chem. Soc. Rev.*, 41(6), 2193-2221. <https://doi.org/10.1039/C1cs15203c>
- [5]. Bahrami, A., Mehr, M., Driel, W., Zhang, K. (2021). Facile Synthesis Of Ag Nanowire/TiO₂ And Ag Nanowire/TiO₂/Go Nanocomposites For Photocatalytic Degradation Of Rhodamine B. *Materials*, 4(14), 763. <https://doi.org/10.3390/ma14040763>
- [6]. Yan, Y., Guo, H., Wang, Z., Li, X., Yan, G., Wang, J. (2020). Electrospinning-Enabled Si/C Nanofibers With Dual Modification As Anode Materials For High-Performance Lithium-Ion Batteries. *Acta Metallurgica Sinica (English Letters)*, 3(34), 329-336. <https://doi.org/10.1007/S40195-020-01087-Z>
- [7]. Karakoti, A., Das, S., Thevuthasan, S., Seal, S. (2011). Pegylated Inorganic Nanoparticles. *Angewandte Chemie*, 9(50), 1980-1994. <https://doi.org/10.1002/anie.201002969>

- [8]. Magnone, E., Hwang, J. Y., Shin, M. K., Zhuang, X., Lee, J. M., & Park, J. T. (2022). Al₂O₃-Based Hollow Fiber Membranes Functionalized By Nitrogen-Doped Titanium Dioxide For Photocatalytic Degradation Of Ammonia Gas. *Membranes*, 12(7), 693. <https://doi.org/10.3390/Membranes12070693>
- [9]. Tayel, A., Ramadan, A., Seoud, O. (2018). Titanium Dioxide/Graphene And Titanium Dioxide/Graphene Oxide Nanocomposites: Synthesis, Characterization And Photocatalytic Applications For Water Decontamination. *Catalysts*, 11(8), 491. <https://doi.org/10.3390/Catal110491>
- [10]. Dey, A., Karan, S., & De, S. (2010). Molecular Interaction And Ionic Conductivity Of Polyethylene Oxide– Nanocomposites. *Journal Of Physics And Chemistry Of Solids*, 71(3), 329–335. <https://doi.org/10.1016/j.jpcs.2009.12.085>
- [11]. Jiang, Y., Wang, W., Biswas, P., & Fortner, J. D. (2014). Facile Aerosol Synthesis And Characterization Of Ternary Crumpled Graphene–TiO₂–Magnetite Nanocomposites For Advanced Water Treatment. *ACS Applied Materials & Interfaces*, 6(14), 11766–11774. <https://doi.org/10.1021/Am5025275>
- [12]. Purabgola, R., Mayilswamy, N., & Kandasubramanian, B. (2022). Graphene-Based TiO₂ Composites For Photocatalysis & Environmental Remediation: Synthesis And Progress. *Environmental Science And Pollution Research*, 29(22), 32305–32325. <https://doi.org/10.1007/S11356-022-18983-9>
- [13]. Sreekanth, T., Jaipal Reddy, M., & Subba Rao, U. (2001). Polymer Electrolyte System Based On (PEO+KBrO₃) — Its Application As An Electrochemical Cell. *Journal Of Power Sources*, 93(1–2), 268–272. [https://doi.org/10.1016/S0378-7753\(00\)00558-9](https://doi.org/10.1016/S0378-7753(00)00558-9)
- [14]. Tan, L. L., Ong, W. J., Chai, S. P., Goh, B. T., & Mohamed, A. R. (2015). Visible-Light-Active Oxygen-Rich TiO₂ Decorated 2D Graphene Oxide With Enhanced Photocatalytic Activity Toward Carbon Dioxide Reduction. *Applied Catalysis B: Environmental*, 179, 160–170. <https://doi.org/10.1016/j.apcatb.2015.05.024>
- [15]. Saravanan, R., Karthikeyan, S., Gupta, V. K., Sekaran, G., Narayanan, V., & Stephen, A. J. M. S. (2013). Enhanced Photocatalytic Activity Of ZnO/CuO Nanocomposite For The Degradation Of Textile Dye On Visible Light Illumination. *Materials Science And Engineering: C*, 33(1), 91–98. <https://doi.org/10.1016/j.msec.2012.08.011>
- [16]. Shahrudin, M. Z., Zakaria, N., Junaidi, N. F. D., Alias, N. H., & Othman, N. H. (2016). Study Of The Effectiveness Of Titanium Dioxide (TiO₂) Nanoparticle In Polyethersulfone (PES) Composite Membrane For Removal Of Oil In Oily Wastewater. *Journal Of Applied Membrane Science & Technology*, 19(1). <https://doi.org/10.11113/Amst.V19i1.21>
- [17]. Benchaabane, A., Ben Hamed, Z., Lahmar, A., Sanhoury, M. A., Kouki, F., Zellama, K., Bouchriha, H. (2016). Optical Properties Of P3HT:Tributylphosphine Oxide-Capped CdSe Nanocomposites. *Applied Physics A*, 122(8). <https://doi.org/10.1007/S00339-016-0244-Z>
- [18]. Alzagameem, A., Klein, S. E., Bergs, M., Do, X. T., Korte, I., Dohlen, S., ... & Schulze, M. (2019). Antimicrobial Activity Of Lignin And Lignin-Derived Cellulose And Chitosan Composites Against Selected Pathogenic And Spoilage Microorganisms. *Polymers*, 11(4), 670. <https://doi.org/10.3390/polym11040670>
- [19]. Carrot, C., Bendaoud, A., & Pillon, C. (2015, December 22). *Handbook Of Thermoplastics*. <https://doi.org/10.1201/B19190-4>
- [20]. Lau, G. E., Che Abdullah, C. A., Wan Ahmad, W. A. N., Assaw, S., & Zheng, A. L. T. (2020). Eco-Friendly Photocatalysts For Degradation Of Dyes. *Catalysts*, 10(10), 1129. <https://doi.org/10.3390/Catal10101129>
- [21]. Patil, M. T., Lakshminarasimhan, S. N., & Santhosh, G. (2021). Optical And Thermal Studies Of Host Poly (Methyl Methacrylate) (PMMA) Based Nanocomposites: A Review. *Materials Today: Proceedings*, 46, 2564–2571. <https://doi.org/10.1016/j.matpr.2021.01.840>
- [22]. Benchaabane, A., Ben Hamed, Z., Lahmar, A., Sanhoury, M. A., Kouki, F., Zellama, K., Bouchriha, H. (2016). Optical Properties Of P3HT:Tributylphosphine Oxide-Capped CdSe Nanocomposites. *Applied Physics A*, 122(8). <https://doi.org/10.1007/S00339-016-0244-Z>
- [23]. Yang, W., Song, S., Zhang, C., Liang, W., Dong, X., Luo, Y., & Cai, X. (2018). Enhanced Photocatalytic Oxidation And Biodegradation Of Polyethylene Films With PMMA Grafted TiO₂ As Pro-Oxidant Additives For Plastic Mulch Application. *Polymer Composites*, 39(10), 3409–3417. <https://doi.org/10.1002/Pc.24358>
- [24]. Sreekanth, T., Jaipal Reddy, M., & Subba Rao, U. (2001). Polymer Electrolyte System Based On (PEO+KBrO₃) — Its Application As An Electrochemical Cell. *Journal Of Power Sources*, 93(1–2), 268–272. [https://doi.org/10.1016/S0378-7753\(00\)00558-9](https://doi.org/10.1016/S0378-7753(00)00558-9)